Eur. J. Biochem. *178*, 727–739 (1989)

Conformational analysis of the sialyl$\alpha(2\rightarrow3/6)$*N*-acetyllactosamine structural element occurring in glycoproteins, by two-dimensional NOE ^{1}H-NMR spectroscopy in combination with energy calculations by hard-sphere exo-anomeric and molecular mechanics force-field with hydrogen-bonding potential

Jan BREG[1], Loes M. J. KROON-BATENBURG[1,2], Gérard STRECKER[3], Jean MONTREUIL[3] and Johannes F. G. VLIEGENTHART[1]

[1] Department of Bio-Organic Chemistry, University of Utrecht
[2] Laboratorium voor Kristal- en Structuurchemie, University of Utrecht
[3] Laboratoire de Chimie Biologique, Université des Sciences et Techniques de Lille I, Villeneuve-d'Ascq

(Received July 28, 1988) – EJB 88 0914

The conformation is described of the sialyl$\alpha(2\rightarrow3/6)$*N*-acetyllactosamine structural element, frequently occurring in glycoproteins. NOE spectroscopy of NeuAc$\alpha(2\rightarrow3)$Gal$\beta(1\rightarrow4)$GlcNAc$\beta(1\rightarrow$N)Asn and NeuAc$\alpha(2\rightarrow6)$Gal$\beta(1\rightarrow4)$GlcNAc$\beta(1\rightarrow$N)Asn is presented and for each glycosidic linkage, except for the $\alpha(2\rightarrow6)$-linkage, a number of interglycosidic NOEs are measured. The analysis of these effects is performed using a full relaxation matrix. Analysis of intraresidue NOEs provides a calibration of the calculation method. Hard-sphere exo-anomeric (HSEA) energy calculations indicate a single conformation for the $\beta(1\rightarrow4)$-linkage in both compounds, both being consistent with the NOE data. HSEA and molecular-mechanics force-field with hydrogen-bonding potential energy calculations both indicate the existence of three preferred conformations for the $\alpha(2\rightarrow3)$-linkage. The analysis of the NOE spectra are consistent with a distribution over two or three of these conformations; by combination with the energy diagram for this linkage the existence of onyl a single conformation can be excluded. The NOE spectrum of the compound with the $\alpha(2\rightarrow6)$-linkage indicates a *gt* orientation for the Gal C-6 hydroxymethyl group. On this basis, the HSEA energy calculations for the $\alpha(2\rightarrow6)$-linkage indicate an extended low-energy surface with a number of preferred conformations. The absence of NOEs across this linkage is interpreted in terms of a non-rigid, but overall folded conformation of the NeuAc$\alpha(2\rightarrow6)$Gal$\beta(1\rightarrow4)$GlcNAcβ structural element. This provides an explanation for the shift effects induced by $\alpha(2\rightarrow6)$ attachment of NeuAc to the *N*-acetyllactosamine unit.

The structural elements NeuAc$\alpha(2\rightarrow3)$Gal$\beta(1\rightarrow4)$GlcNAc$\beta(1\rightarrow$. and NeuAc$\alpha(2\rightarrow6)$Gal$\beta(1\rightarrow4)$GlcNAc$\beta(1\rightarrow$. are prominent parts of many sialyl oligosaccharide chains of glycoproteins and are believed to be involved in the biological function [1, 2]. The negative charge of sialic acid is important for the biological functioning of sialyl oligosaccharides, but since in general the conformation of oligosaccharide chains in solution is of major importance for their activity as well, it is important to determine the conformation of the forementioned structural elements. Structural analysis of oligosaccharides has frequently been carried out by ^{1}H-NMR analysis using structural reporter-group chemical shifts [3, 4]. The ^{1}H-NMR shift effects of NeuAc$\alpha(2\rightarrow3)$ attachment to the lactosamine unit are restricted to Gal, whereas introduction of NeuAc in $\alpha(2\rightarrow6)$ linkage induces shift effects on Gal, GlcNAc and even on more remote sugar residues. This has been interpreted as backfolding of the $\alpha(2\rightarrow6)$-linked sialic acid along the chain [4].

The orientation of the NeuAc$\alpha(2\rightarrow3)$Galβ element has been the subject of a previous investigation, wherein the conformation was studied of the ganglioside G_{M1}, i.e. Galβ-$(1\rightarrow3)$GalNAc$\beta(1\rightarrow4)$[NeuAc$\alpha(2\rightarrow3)$]Gal$\beta(1\rightarrow4)$Glc [5]. The conformation of the $\alpha(2\rightarrow3)$-linkage was evaluated from HSEA calculations upon attachment of NeuAc at asialo G_{M1}. The energy calculations indicated two possible conformations for the NeuAc attachment site, one of which was abandoned on the grounds of ^{1}H,^{1}H NOEs obtained from measurements performed in the difference mode [6]. However, in this oligosaccharide NeuAc is $\alpha(2\rightarrow3)$-linked to a Gal residue that is also substituted by βGalNAc at C-4 and the conformational analysis indicated that the βGalNAc unit is extensively and rather strongly bonded through secondary forces to the NeuAc unit. This finding suggests an influence of GalNAc on the actual conformation around the $\alpha(2\rightarrow3)$ linkage, rendering it different from the case wherein NeuAc is linked to terminal Gal.

Here, the conformation is described of glycoasparagines containing sialyl$\alpha(2\rightarrow3)$- or $\alpha(2\rightarrow6)$*N*-acetyllactosamine $\beta(1\rightarrow$N) linked to Asn. These compounds are suitable as models for the title structural elements in larger oligosaccharides, since the structural reporter-group chemical shift

Correspondence to J. F. G. Vliegenthart, Department of Bio-Organic Chemistry, Utrecht University, Transitorium III, P.O. Box 80.075, NL-3508 TB Utrecht, The Netherlands

Abbreviations. 1D, one-dimensional; 2D, two-dimensional; ppm, parts per million; NOESY, nuclear Overhauser effect spectroscopy; HSEA, hard-sphere exo-anomeric; COSY, correlated spectroscopy; 2D-*J*, two-dimensional *J*-resolved; MM2HB, molecular-mechanics force-field with hydrogen-bonding potential; TPPI, time-proportional phase increment.

effects upon sialylation are highly comparable to those observed in larger oligosaccharides [3]. The conformation of the model compounds is determined from ^{1}H-NMR cross-relaxation, expressed in NOEs. The latter effects are of dipolar origin and are indicative of close distance, i.e. less than about 0.4 nm. In the present report they are measured as crosspeaks in 2D-NOE (NOESY) spectra. The application of the 2D, rather than the 1D mode allows determination of all transient NOEs in one experiment. Furthermore, in crowded spectra the determination of NOEs by difference spectroscopy will become unreliable due to perturbation of neighbouring signals. This is relevant for larger oligosaccharides and glycopeptides, with inherent spectral overlap.

It is generally accepted that most monosaccharide residues in oligosaccharides have a relatively non-varying rigid structure. Consequently, the overall oligosaccharide conformation is determined by the orientation of the constituting monosaccharides with respect to one another, expressed in interglycosidic torsion angles. Therefore, quantitative interpretation of interglycosidic NOEs to proton-proton distances renders the oligosaccharide conformation in terms of interglycosidic torsion angles. In this report the conformation is determined mainly from a quantitative analysis of 2D-NOE data, in combination with the results of HSEA and MM2HB energy calculations.

MATERIALS AND METHODS

Isolation of glycopeptides

Compounds I (24 mg), II (14 mg) and III (5 mg) (see Scheme 1) were isolated from the urine of a patient with aspartylglucosaminuria as described before [3, 7].

I Galβ(1→4)GlcNAcβ(1→N)Asn

II Galβ(1→4)GlcNAcβ(1→N)Asn
/
NeuAcα(2→3)

III NeuAcα(2→6)
\
Galβ(1→4)GlcNAcβ(1→N)Asn

Scheme 1. *Structures of the glyco-asparagines as isolated from a patient with aspartyl-glucosaminuria and investigated in this report*

^{1}H- and ^{13}C-NMR spectroscopy

500-MHz ^{1}H-NMR experiments were performed on a Bruker AM-500 spectrometer (SON hf-NMR facility, Department of Biophysical Chemistry, University of Nijmegen, the Netherlands, or Department of NMR Spectroscopy, University of Utrecht) equipped with an Aspect-3000 computer. Prior to analysis, the samples were repeatedly treated with ^2H_2O at p^{2}H 7 and at room temperature, with intermediate lyophilization, and finally dissolved in 0.4 ml 99.96% ^2H_2O (Aldrich), rendering concentrations for I, II and III of about 115 mM, 44 mM and 16 mM, respectively. The experiments were performed at a probe temperature of 27°C unless stated otherwise. Chemical shifts (δ) are expressed in ppm downfield from 4,4-dimethyl-4-silapentane-1-sulfonate, but were actually measured by reference to internal acetone (set to δ = 2.225 ppm in ^2H_2O at all temperatures).

For the 2D *J*-resolved ^{1}H-NMR spectra, the usual pulse sequence was employed [8, 9], but the HDO signal was suppressed by the inversion-recovery method, i.e. after the recycle delay a composite 180° pulse and an appropriate relaxation delay were inserted to achieve zero HDO magnetization at the time of the first 90° pulse [10]. Prior to Fourier transformation, the resolution was enhanced in ω_1 and ω_2 by non-shifted sine functions and by zerofilling. ^{1}H-^{1}H 2D-shift-correlated (COSY) experiments were performed at 8°C and the spectra were obtained by a three-pulse sequence, 90° – t_1 – 90° – 90° – acq, which, by adequate phase-cycling of receiver and detection-pulse resulted in coherence transfer through a double quantum filter [11]. Phase-sensitive handling of the data in ω_1 became possible by application of the time-proportional phase increment (TPPI) [12]. A 640 × 4K data matrix was obtained, which was zero-filled to 2K × 4K prior to Fourier transformation. Resolution enhancement in ω_2 and suppression of truncation artifacts in ω_1 was obtained by a $\pi/4$ shifted and a non-shifted sine-squared-bell function in t_2 and t_1, respectively.

Prior to the NOESY experiments, the samples were degassed in the NMR tube by repeated evacuation, allowing argon to replace the air in the tube, sealed under argon and then (D_6) acetone (99.8% D, Merck) was added for a deuterium lock (5% by vol.). NOESY experiments [13, 14] were performed at 4°C and spectra were obtained with mixing periods of 0.25 s, 0.33 s or 0.45 s (compound II), or 0.4 s (compound III), and a relaxation delay of 2 s between consecutive scans. Appropriate phase-cycling of the detection pulse and receiver allowed for selection of correlations through magnetization exchange only, with the exception of zero-quantum coherence [15]. Phase-sensitive handling of data in ω_1 was possible by application of TPPI (compound II) or by placing the spectral offset outside the spectrum (compound III). A 400 × 4K data matrix was obtained that was zero-filled to 2K × 4K prior to Fourier transformation. Sine-squared weighting functions, $\pi/3$ shifted, were applied to enhance the resolution in ω_2 and to suppress truncation in ω_1. These were in fact moderate resolution enhancements which did not distort relative peak intensities. NOESY crosspeaks intensities were obtained by adding ω_1 subspectra contributing to a specific signal and are expressed as a percentage of the total intensity for each signal in ω_1. Compared to a single cross-section, this not only improves the signal/noise ratio, but also annuls contributions from (dispersive) zero-quantum coherence transfer [15].

50-MHz ^{13}C-NMR experiments were performed at 27°C on a Bruker WM-200 spectrometer (SON hf-NMR facility) equipped with an Aspect-2000 computer. ^{13}C-NMR chemical shifts (δ) are expressed in ppm relative to internal acetone at δ = 31.55 ppm, with an accuracy of 0.02 ppm. The 125-MHz ^{13}C-NMR spectrum of III was obtained on a Bruker AM-500 spectrometer (K. Bock, Lyngby, Denmark). ^{13}C-NMR T_1-relaxation values were determined by the inversion-recovery method [16] with a three-parameter fit for the recovered intensities. The interpretation of the T_1 values in terms of rotational mobility was according to [17]. Briefly, for carbohydrates in solution, the ^{13}C relaxation is governed by dipolar coupling between covalent bonded H and C spins. Assuming isotropic rotational motion, the T_1-relaxation time is described by

$$\frac{1}{T_1^c} = \left(\frac{\mu_0}{2\pi}\right)^2 \frac{\hbar^2 N \gamma_C^2 \gamma_H^2}{10 r_{C-H}^6} \times \left\{ \frac{\tau_c}{1 + (\omega_H - \omega_C)^2 \tau_c^2} + \frac{3\tau_c}{1 + \omega_C^2 \tau_c^2} + \frac{6\tau_c}{1 + (\omega_H + \omega_C)^2 \tau_c^2} \right\}$$

wherein μ_0 is the magnetic permeability of vacuum, $\hbar$ is Planck's constant divided by 2π, γ_C and γ_H are the carbon and proton gyromagnetic ratio, respectively, τ_c is the rotational correlation time, r_{C-H} is the proton-carbon distance, and N is the number of covalently attached protons. In the analysis, the proton-carbon distances were assumed to be 0.11 nm.

Calculation of NOE crosspeak intensities

When only low amounts of materials are available, a prolonged mixing time is needed to obtain an adequate signal/noise ratio in NOESY experiments. However, this precludes analysis using initial NOE built-up rates [18] and analysis should be done using the full relaxation matrix [19]. For a multi-spin system, the integrated intensity of a crosspeak between two protons i and j in a NOESY spectrum is proportional [15] to the mixing coefficient a_{ij}, between protons i and j

$$a_{ij}(\tau_m) \approx [\exp(-\mathbf{R}\tau_m)]_{ij}$$

wherein τ_m is the mixing time and $\mathbf{R}$ is the relaxation matrix describing the cross-relaxation between all protons. This equation may be evaluated numerically [19] by rewriting the matrix of the mixing coefficients, $\mathbf{a}$, as

$$\mathbf{a}(\tau_m) = \boldsymbol{\chi} \exp(-\boldsymbol{\lambda}\tau_m)\boldsymbol{\chi}^{-1}$$

wherein $\boldsymbol{\chi}$ and $\boldsymbol{\lambda}$ are the matrices containing the eigenvectors and eigenvalues, respectively, of the relaxation matrix. The elements R_{ii} and R_{ij} of the relaxation matrix are written as

$$R_{ii} = \Sigma_j (W_0^{ij} + 2W_1^{ij} + W_2^{ij}) + R_{li}$$

$$R_{ij} = (W_2^{ij} - W_0^{ij})$$

wherein W_0, W_1 and W_2 are the zero-, single-, and double-quantum transition probabilities, and R_{li} is a leak relaxation of nuclei i to external sources. The transition probabilities are in turn written as

$$W_1^{ij} = 1.5\, q_{ij}\, J(\omega_i)$$

$$W_0^{ij} = q_{ij}\, J(\omega_i - \omega_j)$$

$$W_2^{ij} = 6\, q_{ij}\, J(\omega_i + \omega_j)$$

wherein $J(\omega)$ is the spectral density function describing the motion of the dipolar coupled nuclei. $J(\omega)$ is retrieved from the model of motion that is assumed for the molecule; it contains one or more rotational correlation times τ_c describing the rates of motion. Here, isotropic motion is assumed for the complete molecule, described by a single τ_c. In that case q_{ij} is given by

$$q_{ij} = 0.1\, \gamma_i^2 \gamma_j^2 (h/2\pi)^2 r_{ij}^{-6}$$

which expression contains the distance between protons i and j. In the present analysis the total intensity of the added ω_1 cross-sections containing diagonal and crosspeaks was scaled to 100%. By scaling to 100% at each mixing time, the effect of net relaxation, including leak relaxation, is eliminated. In fact each row i of the matrix $\mathbf{a}$ is multiplied by $\exp(\tau_m/T_{1i})$.

Energy calculations and conformational analysis

The HSEA energy calculations [20] were performed for the two trisaccharide moieties in II and III, with GlcNAc in the β-anomeric form. In these calculations the constituting monosaccharides were taken as rigid structures with each glycosidic angle set to 117°, leaving as variables determining the oligosaccharide conformation only the torsion angles ϕ and ψ. For a 1−4 linkage ϕ is defined by the atoms H1-C1-O1-C4 and ψ by C1-O1-C4-H4; for NeuAc ϕ is defined by the atoms C1-C2-O2-C3 (see Fig. 1). Three preferred values are assumed for the torsion angle across the C5-C6 bond for Gal and GlcNAc, i.e. $\omega = 55$ (*gg*), $\omega = -175$ (*gt*) or $\omega = -65$ (*tg*), wherein ω is defined by the atoms O6-C6-C5-C4. In HSEA energy calculations only non-bonded interactions, described by the Kitaychorodsky potential [21], are taken into account, together with a contribution from a torsion potential across ϕ, that accounts for the exo-anomeric effect [22]. The coordinates for the constituting monosaccharides were taken from the crystal neutron diffraction data of methyl β-D-galactopyranoside [23] and X-ray crystal data of 2-acetamido-2-deoxy-β-D-glucopyranose [24] and 1,2-Me_2-α-Neu5Ac (Kroon-Batenburg and Kooiman, unpublished results), with the proton-carbon distances set to 0.11 nm. In the conformation of the latter molecule the glycerol side chain is involved in two strong intra-residue hydrogen bonds, i.e. between the hydroxyl group of C-7 and the carbonyl group of the *N*-acetyl side chain and between the hydroxyl group of C-8 and one of the carboxyl oxygen atoms (Kroon-Batenburg and Kooiman, unpublished results). The carboxyl group is in plane with C-2 and O-2, deviating from previous data [5], but the orientation of the glycerol side chain is identical to that originally proposed by Brown et al. [26]. The energy diagrams for the ϕ/ψ space were obtained with a 5° grid. The molecular-mechanics energy calculations were performed using standard software, MM2 [27], extended with an empirical potential describing hydrogen-bond formation, MM2HB [28]. With MM2HB in addition to non-bonded interactions, electrostatic contributions are also taken into acount, and a special hydrogen bond potential assures proper hydrogen bond geometries. In contrast to the HSEA calculations, the MM2HB calculation includes full optimization of the molecular geometry. In this way the calculations account for perturbations in the conformations of the two-monosaccharide structure for each ϕ/ψ value, so they are allowed to have an optimal interaction and no unrealistically large repulsion at certain ϕ/ψ values. MM2HB calculations were performed on 1-Me-βGal and 1-Me-βGlcNAc to gain insight into the orientation of their

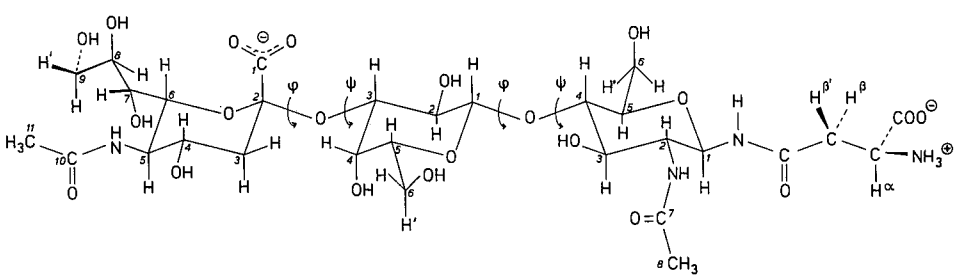

Fig. 1. *Structure of II.* The atoms in the molecule are numbered according to the skeleton atoms

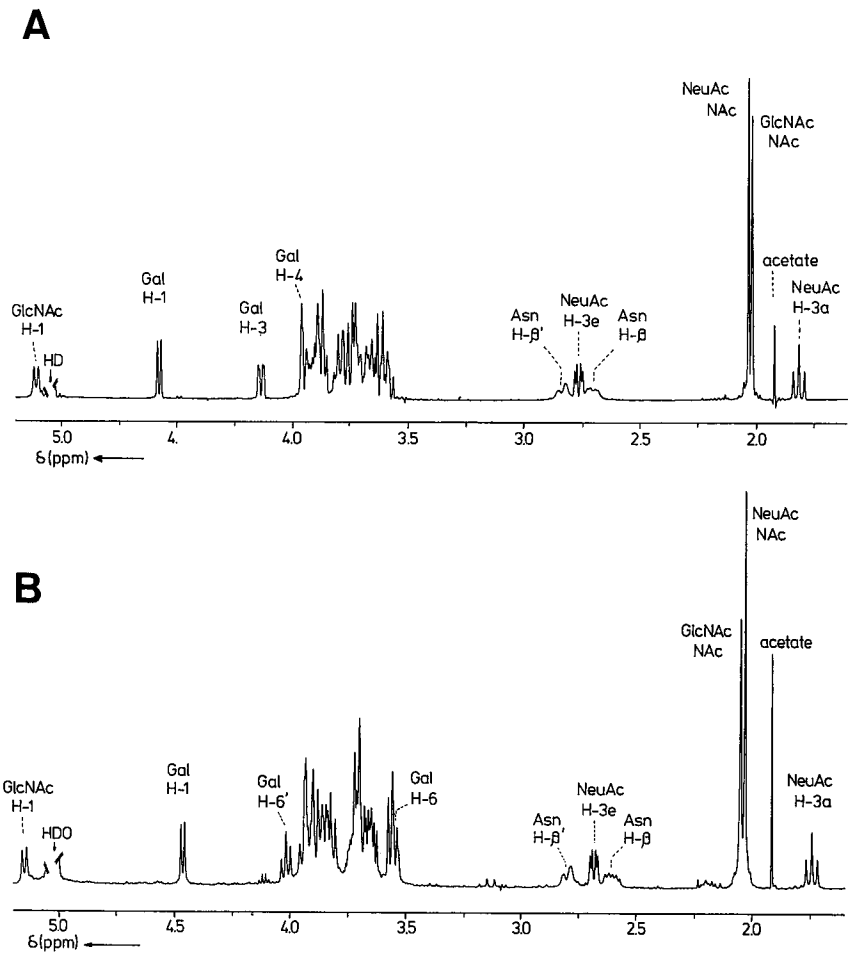

Fig. 2. *500-MHz ^{1}H-NMR spectra of (A) II and (B) III*

hydroxymethyl groups, and on the disaccharide 1-Me-Neu5Ac-α(2→3)Galβ.

The NOESY crosspeak intensities are strongly dependent on τ_c. An indication for its value was given by ^{13}C T_1-relaxation data, but a definitive value for τ_c was obtained from a fit of the calculated with observed intraresidue crosspeaks. The calculated crosspeak intensities were evaluated as weighted deviations from the observed intensities (Δrms_w), according to the expression

$$\Delta\text{rms}_w = \sqrt{\frac{\Sigma w_{ij}(a_{ij} - a_{ij}^o)^2}{\Sigma w_{ij}}}$$

wherein a_{ij}^o is the observed intensity and $w_{ij} = 1/\sigma^2$, with σ_{ij} being the estimated absolute error for a_{ij}^o. σ_{ij} was estimated separately for each a_{ij}^o and ranged between 1.5−0.2% for NOE intensities of 25% and 0.6%, respectively. In the absence of a detectable crosspeak, a_{ij}^o was assumed to be 0, with σ_{ij} set to the detection level (≈0.2%). In case of an inter-glycosidic NOE that was essential for the conformation analysis, but for which the crosspeak overlapped, a_{ij}^o could usually be estimated, but σ_{ij} was taken much higher. The analysis of the interglycosidic NOEs was performed in several stages. First, for each linkage a single conformation was established by a 5° grid search of ϕ and ψ for the closest correspondence between calculated and observed inter-glycosidic NOE intensities. This result was compared to the energy profile for the linkage. Secondly, the inter-glycosidic NOE crosspeak intensities were calculated for the linkage conformations corresponding to energy minima. Thirdly, an improved correspondence was obtained between calculated and observed NOE intensities by calculating the NOE peak intensities from a rate matrix to which more than one conformation contributed.

RESULTS AND DISCUSSION

The 500-MHz ^{1}H-NMR spectra of I, II and III (see Fig. 2), together with the assignment of the structural-reporter group resonances have been reported before [3, 7]. The complete unraveling of the ^{1}H spectra of I (earlier obtained by 1D-NMR methods [3]), II and III is obtained by ^{1}H-^{1}H COSY, combined with 2D *J*-resolved spectroscopy (Table 1). To comply with the NOESY experiment, the COSY spectra for II and III have been obtained at 8 °C, although the shift differences for spectra obtained at 8 °C and 27 °C, respectively, are only small. The 2D-*J* spectrum of II is given in Fig. 3; an expansion of the region between 4.1−3.5 ppm of the COSY spectrum of II (Fig. 4) displays in detail the shift correlations between ring-proton chemical shifts in the central part of the spectrum. The strong coupling ($\Delta\delta \leq J$) between GlcNAc H-3 and H-4 and between Gal H-5, H-6 and H-6′ results in distorted multiplet crosspeaks for these protons and causes virtual coupling on neighbouring protons [29]. The many artifacts in the 2D-*J* spectra, caused by strong coupling, are exemplified by the clearly observed 'extra' multiplet at the average shift position of Asn β and β′ (see Fig. 3).

Table 1. *^{1}H-NMR chemical shifts of I, II and III*
Chemical shifts are measured in neutral ^2H_2O solution at 8 °C for II and III, 27 °C for I, and are expressed relative to internal acetone (δ = 2.225 ppm). Coupling constants (in parentheses) are as determined from 2D-*J* spectra or from spectral simulation in case of strong coupling (see text)

Residue	Proton (*J*)	δ(*J*) for		
		I	II	III
		ppm (Hz)		
GlcNAc	H-1 ($J_{1,2}$)	5.107 (9.8)	5.107 (9.7)	5.134 (9.8)
	H-2 ($J_{2,3}$)	3.890 (10.0)	3.895 (10.4)	3.881 (10.4)
	H-3 ($J_{3,4}$)	3.778 (8.8)	3.764 (9)[b]	3.802 (9)[b]
	H-4 ($J_{4,5}$)	3.754 (10.2)	3.777 (10)[b]	3.682[a] (10)[b]
	H-5 ($J_{5,6}$)	3.670 (2.3)	3.661 (2.3)	3.685[a] (2)[b]
	H-6 ($J_{5,6'}$)	3.941 (4.6)	3.946 (4.6)	3.929 (5.7)
	H-6′ ($J_{6,6'}$)	3.837 (−12.3)	3.863 (−12.4)	3.828 (−12.5)
	NAc	2.018	2.014	2.042
Gal	H-1 ($J_{1,2}$)	4.481 (7.9)	4.572 (7.8)	4.447 (7.9)
	H-2 ($J_{2,3}$)	3.549 (9.9)	3.582 (9.9)	3.537 (10.0)
	H-3 ($J_{3,4}$)	3.667 (3.4)	4.128 (3.1)	3.668 (3.6)
	H-4 ($J_{4,5}$)	3.927 (0.9)	3.957 (1.5)	3.917 (1.6)
	H-5 ($J_{5,6}$)	3.708 (3.5)[b]	3.72 (3.5)[b]	3.825 (3.6)
	H-6 ($J_{5,6'}$)	3.742 (8.5)[b]	3.73 (8.5)[b]	3.528 (9.2)
	H-6′ ($J_{6,6'}$)	3.785 (−11.5)[b]	3.76 (−11.5)[b]	3.996 (−10.4)
NeuAc	H-3a ($J_{3a,3e}$)		1.801 (−12.8)	1.717 (−12.5)
	H-3e ($J_{3a,4}$)		2.774 (11.6)	2.662 (12.0)
	H-4 ($J_{3e,4}$)		3.684 (4.6)	3.639 (4.9)
	H-5 ($J_{4,5}$)		3.854 (9.6)	3.805 (9.9)
	H-6 ($J_{5,6}$)		3.618 (10.5)	3.694 (10.6)
	H-7 ($J_{6,7}$)		3.593 (1.8)	3.547 (1.8)
	H-8 ($J_{7,8}$)		3.903 (9.2)	3.889 (9.0)
	H-9 ($J_{8,9}$)		3.867 (2.3)	3.875 (2.3)
	H-9′ ($J_{8,9'}$)		3.633 (6.7)	3.627 (6.6)
	CH_3 ($J_{9,9'}$)		2.028 (−12.3)	2.028 (−12.2)
Asn	Hα ($J_{\alpha,\beta}$)	3.985 (6.7)	3.993 (6.7)	3.987 (6.7)
	Hβ ($J_{\alpha,\beta'}$)	2.875 (4.5)	2.879 (4.5)	2.866 (4.5)
	Hβ' ($J_{\beta,\beta'}$)	2.942 (−17.2)	2.950 (−17.2)	2.955 (−17.2)

[a] Position determined from NOESY spectrum.
[b] Approximate value.

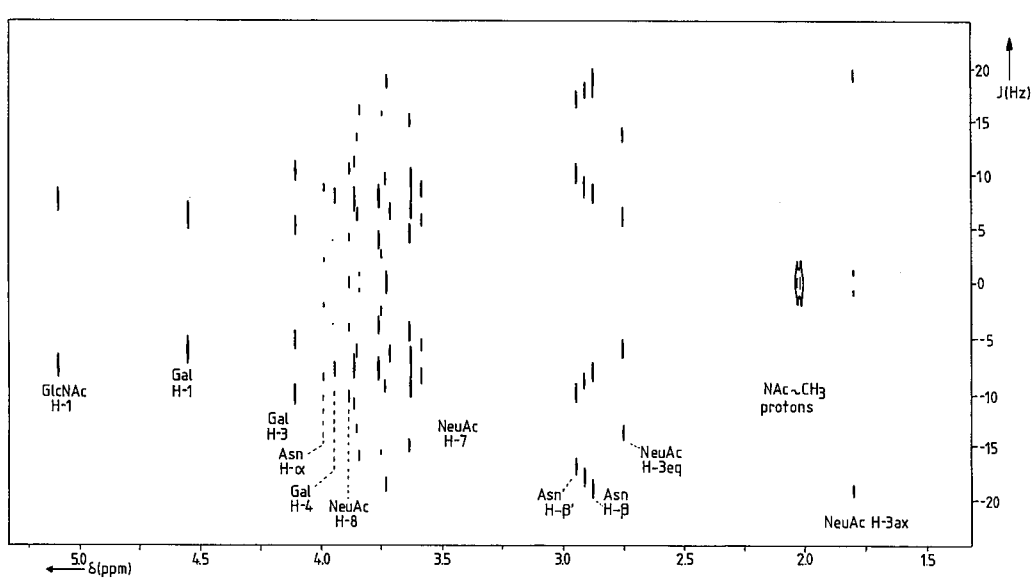

Fig. 3. *500-MHz 2D J-resolved spectrum of II.* The spectrum obtained after the Fourier transformation has been tilted 45° and symmetrized around $J = 0$

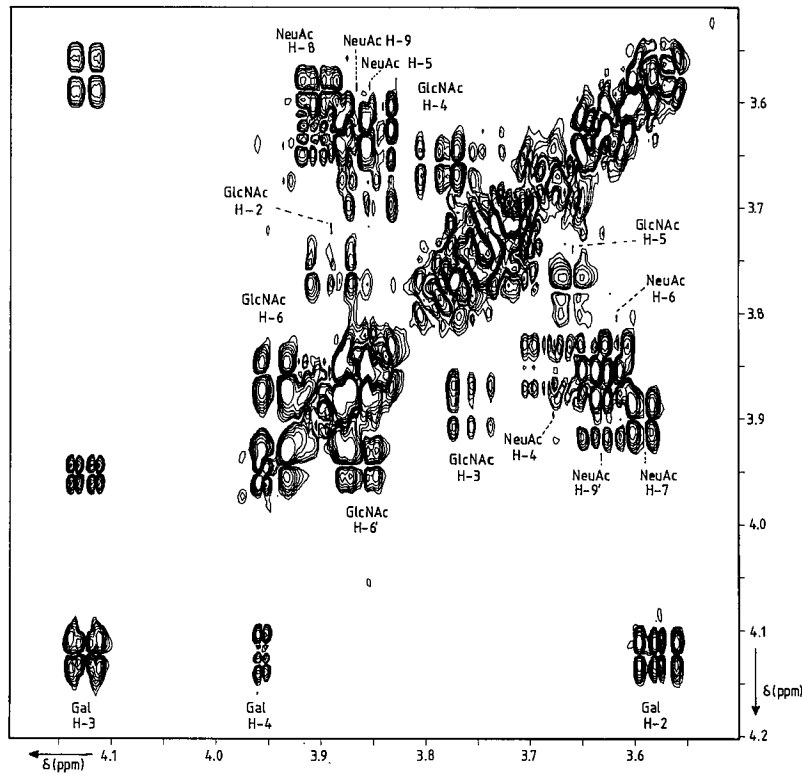

Fig. 4. *500-MHz ^1H-^1H COSY spectrum of II at 8°C.* Only the expanded region of skeleton protons is shown. The assigned crosspeaks denote shift positions along ω_2. The Gal H-4/H-5 crosspeak is below the lowest level of the contour plot, while the Gal H-5, H-6 and H-6′ peaks are all in the region between 3.70 and 3.82 ppm

Extensions of I with NeuAc in α(2→3) linkage leading to II, results in major chemical-shift effects on Gal H-1, H-2, H-3 and H-4 of $\Delta\delta$ +0.091, +0.033, +0.461 and +0.030 ppm, respectively. No significant chemical shift effects are observed on GlcNAc proton resonances. Comparison of the ^{1}H-NMR data in I and III shows that the NeuAcα(2→6) linkage induces chemical shift changes not only for Gal H-1, H-5, H-6 and H-6′ of $\Delta\delta$ −0.034, +0.117, −0.214 and +0.211 ppm, respectively, but also for GlcNAc H-1, H-3, H-4 and NAc of +0.027, +0.024, −0.072 and +0.024 ppm, respectively. The shift effects on GlcNAc H-1 and NAc are in accordance with those observed for larger oligosaccharides containing the same structural element [3]. As such these chemical-shift effects suggest some interaction between the NeuAc and the GlcNAc residue for the α(2→6) linkage, distinct from the α(2→3) case. The chemical shift effects for Gal H-6 and H-6′ of III compared to I are strongly upfield and downfield, respectively, indicating distinct shielding effects for Gal H-6 and deshielding effects for Gal H-6′ of III. This suggests a specific orientation of the NeuAc residue with respect to each of the Gal H-6 protons.

Hydroxymethyl-group orientation

To gain insight into the orientation of the hydroxymethyl groups in Gal and GlcNAc, an MM2HB energy profile is calculated for rotation of the hydroxymethyl group about the C5-C6 linkage (see Fig. 5). To prevent any energy contributions from intra-molecular hydrogen-bond formation, e.g. between the OH group at C-6 and the ring oxygen, the C-6 hydroxyl proton has been oriented away from the remaining of the molecule. In calculations wherein such hydrogen-bond formations are allowed, only weak bonds are formed that are not expected to hold in the presence of water. Each energy profile shows three local minima, at the *gg*, *gt* and *tg* orientation. Of these three orientations, *gg* and *tg* for Gal and GlcNAc, respectively, correspond to a *syn*-axial position of the hydroxyl groups of C-4 and C-6. The actual population distribution among the several rotamers is calculated from the observed coupling constants $J_{5,6}$ and $j_{5,6'}$ for Gal and GlcNAc. For each rotamer, $J_{5,6}$ and $J_{5,6'}$ are calculated using modified Karplus equations [30] and the observed couplings are expressed as the sum of these coupling constants, weighted by their population. Taking into acount the energy levels of the respective rotamers, the *gg*, *gt* and *tg* conformers for Gal are populated as 0.10:0.80:0.10 (I and II) or 0.00:0.08:0.15 (III). The predominance of the *gt* orientation for Gal is in accordance with ^{1}H-NMR spectra of (6*R*)- and (6*S*)-(6-^{2}H)-Gal [31]. Therefore in all calculations the *gt* orientation is used for Gal. For III the same orientation is independently deduced from the NOESY spectrum (see below). From the forementioned energy profiles it follows that for GlcNAc the *tg* orientation is minimally occupied, rendering the *gg*, *gt* and *tg* conformers to be populated 0.65:0.35:0.00 (I and II) or 0.50:0.50:0.00 (III). In all further calculations the *gg* orientation is used for GlcNAc, which is in accordance with the predominance of the *gg* orientation for GlcNAc as determined from ^{1}H-NMR spectra of (6*R*)- and (6*S*)-(6-^{2}H)GlcNAc [32].

For the calculation of the NOE intensities, τ_c is of major importance; an estimate for its value is obtained from ^{13}C-NMR T_1 relaxation experiments. The ^{13}C-NMR spectra of I, II and III are straightforwardly assigned using chemical shifts of similar compounds [33, 34] (see Table 2). Analogously to ^{1}H-NMR, significant ^{13}C-NMR long-range shift effects are induced by NeuAc in α(2→6)-linkage, i.e. down-field shift effects of GlcNAc C-4 and CH_3 of 2.15 ppm and 0.11 ppm,

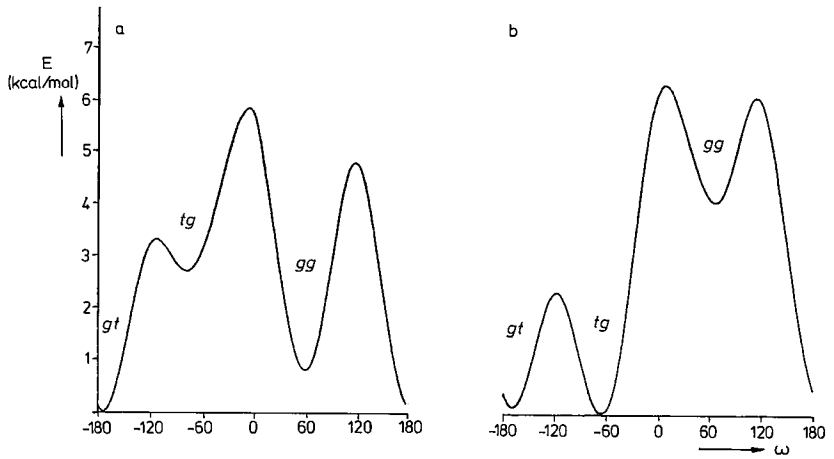

Fig. 5. *MM2HB calculated energy profiles for rotation of the Gal and GlcNAc hydroxymethyl groups around their respective C5-C6 linkages for (a) methyl-β-D-glucose and (b) methyl-β-D-galactose.* The C-6 hydroxyl proton has been oriented away from the remainder of the molecule. 7 kcal/mol ≡ 29 kJ/mol

Table 2. *^{13}C-NMR chemical shift data of I, II and III*
Chemical shifts were measured in neutral ^2H_2O solutions at 27°C, relative to internal acetone (δ = 31.55 ppm). n.d. = not determined

Residue	Carbon	δ for		
		I	II	III
		ppm		
GlcNAc	C-1	79.42	79.48	79.31
	C-2	54.99	55.02	54.82
	C-3	74.16	74.18	74.28
	C-4	79.28	79.08	81.43
	C-5	77.80	77.81	77.51
	C-6	61.20	61.17	61.43
	CH_3	23.40	23.37	23.51
Gal	C-1	104.17	103.88	104.83
	C-2	72.28	70.70	72.06
	C-3	73.85	76.80	73.90
	C-4	69.89	68.81	69.74
	C-5	76.69	76.52	75.02
	C-6	62.35	62.37	64.72
NeuAc	C-1		n.d.	n.d.
	C-2		101.14	101.53
	C-3		40.96	41.43
	C-4		69.68	69.74
	C-5		53.01	53.21
	C-6		74.18	73.73
	C-7		69.44	69.59
	C-8		73.10	73.06
	C-9		63.92	64.00
	CH_3		23.37	23.35
	COO^-		n.d.	n.d.
Asn	C_α	52.32	53.01	55.88
	C_β	36.39	38.31	38.78
	C_γ	n.d.	n.d.	n.d.
	COO^-	n.d.	n.d.	n.d.

Table 3. *50-MHz ^{13}C-NMR T_1 relaxation values at 27°C for I and II*
In NT_1, N is the number of attached protons. n.d. = not determined

Residue	Carbon	NT_1 for	
		I	II
		s	
GlcNAc	1	0.29	0.26
	2	0.32	0.24
	3	0.31	0.24
	4	0.30	0.23
	5	0.31	0.26
	6	0.32	0.24
	NAc	2.25	n.d.
Gal	1	0.33	0.23
	2	0.33	0.23
	3	0.38	0.23
	4	0.29	0.19
	5	0.34	0.21
	6	0.54	0.40
NeuAc	COO^-		n.d.
	2		n.d.
	3		0.24
	4		0.22
	5		0.22
	6		0.23
	7		0.21
	8		0.22
	9		0.42
	NAc		n.d.

respectively. Due to the limited amount of material of compound III, T_1 relaxation measurements have only been performed for I and II, both at 27°C (see Table 3). According to the average T_1 for Gal and NeuAc in II, τ_c of this molecule is 0.22 ns; τ_c for GlcNAc appears to be slightly smaller, 0.2 ns. The NOESY experiments for II and III have actually been performed at 4°C and a value of 0.44 ns is expected [35] for the analysis of the NOE data. The same change of τ_c when decreasing the temperature from 27°C to 4°C was independently determined from ^{13}C-relaxation measurement for sialyl-α(2→3)lactose. ^{13}C-relaxation data for sialyl-α(2→3) and -α(2→6)lactose (unpublished results) do not point to major differences between T_1 values for skeleton carbons of these compounds, suggesting identical overall molecular mobility for II and III. For compounds I and II the Gal hydroxymethyl group has an increased mobility with respect to the ring carbons, contrary to GlcNAc (see Table 3). This is ascribed to the higher energy barrier between the GlcNAc

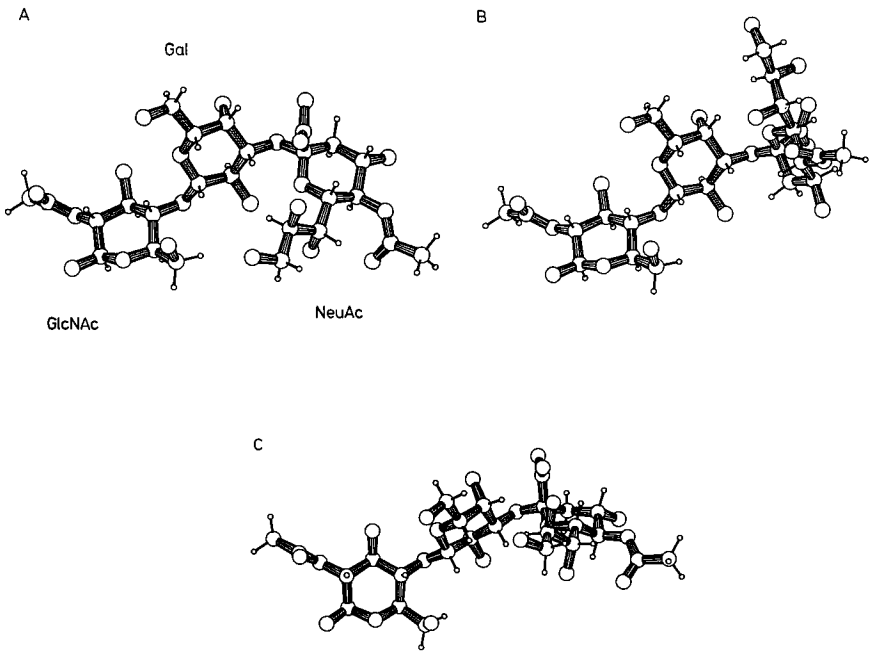

Fig. 6. *Conformations of compound II calculated using the HSEA energy format.* For the $\beta(1\rightarrow4)$ linkage, $\phi/\psi = 55°/5°$ and for the $\alpha(2\rightarrow3)$ linkage, $\phi/\psi = 290°/5°$ (A), $200°/-20°$ (B) or $265°/-45°$ (C). Asn has been omitted from the figure

gg and *gt* conformer ($\approx$17 kJ/mol) compared to that between the Gal *gt* and *tg* conformer ($\approx$9.2 kJ/mol, see Fig. 5). The mobility of Gal C-6 of sialyl-$\alpha(2\rightarrow6)$ lactose is identical to that of the rest of the Gal skeleton carbons, a situation which probably also occurs in III.

For NeuAc in II, the mobility of the glycerol side chain, as indicated by the relaxation data, is the same as reported earlier for sialyl-$\alpha(2\rightarrow3)$ and -$\alpha(2\rightarrow6)$lactose [36], i.e. an increased mobility of C-9 with respect to the ring atoms, but not of C-7 and C-8. The latter restricted mobility was reported before [37] and is in accordance with the hydrogen bonds observed in the crystal structure of 1,2-Me_2-α-Neu5Ac; these bonds appear therefore to be retained in solution, keeping the glycerol side chain in a rigid orientation. The two hydrogen bonds can also be demonstrated by MM2HB calculations for the disaccharide NeuAc$\alpha(2\rightarrow3)$Galβ; the formation of these hydrogen bonds is not accompanied by any significant change of the orientation of the glycerol side chain. This justifies the use of the fixed molecular model for NeuAc in the HSEA calculations and in the analysis of the NOE data.

Conformation of II, with NeuAc in $\alpha(2\rightarrow3)$-linkage

The analysis of the NOE data is preceded by HSEA energy calculations for both glycosidic linkages in II. The HSEA calculations indicate for the Gal$\beta(1\rightarrow4)$GlcNAc linkage a minimum at ϕ and ψ values of 55° and 5°, respectively. For the NeuAc$\alpha(2\rightarrow3)$Gal linkage three local minimum-energy conformations are obtained, at ϕ/ψ values of 290°/5°, 200°/$-20°$ and 265°/$-45°$ (denoted A, B and C, respectively, see Fig. 6), with relative energies 0, 2.5 and 13.8 kJ/mol, respectively. According to these calculations the orientation of the $\beta(1\rightarrow4)$-linkage is not influenced by the presence of NeuAc and vice versa the orientation of the $\alpha(2\rightarrow3)$-linkage not by GlcNAc. MM2HB calculations for the $\alpha(2\rightarrow3)$-linkage point to local-energy-minimum conformations at $\phi/\psi = 203°/-22°$ and 259°/$-56°$ (denoted B′ and C′, respectively), nearly coinciding with B and C, respectively, with relative energies of

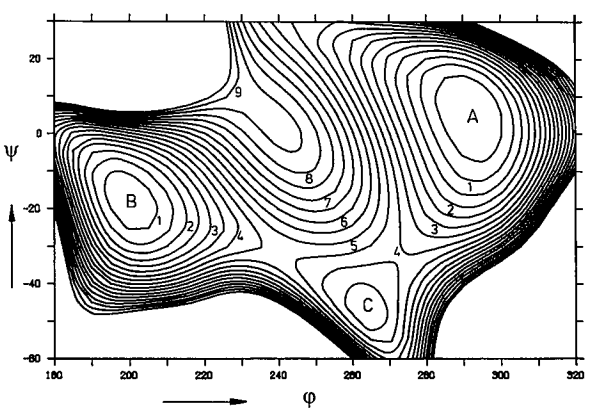

Fig. 7. *Energy profile calculated according to the HSEA format for part of the ϕ/ω space of the NeuAc$\alpha(2\rightarrow3)$Gal linkage for II.* The indicated levels are 0.5 kcal/mol (2.1 kJ/mol) apart and energies more than 10 kcal/mol (42 kJ/mol) above the minimum have been omitted

0 and 9.6 kJ/mol (see Fig. 7). Two additional conformations are found at $\phi/\psi = 298°/3°$ and $296°/-18°$ (denoted A′ and A″), with relative energies of 13.4 and 14.2 kJ/mol. The last two conformations are both close to conformation A and indicate this minimum to be broader than B and C. Both the HSEA and MM2HB energy models therefore point to the existence of three favoured orientations for the NeuAcα-$(2\rightarrow3)$Galβ-linkage, separated by distinct energy barriers. The relative energy levels for the conformations depend on the energy model and they may change even further when energy contributions from charge and solvent are taken into account. The positions of the minima are largely determined by steric repulsion and it is expected that these will not change much when more elaborate energy evaluations are employed. In consequence, all conformations in Fig. 7 with an energy 42 kJ/mol higher than the minimum are excluded as possible conformation due to severe steric hindrance. The local minimum-energy conformations A and B, for the NeuAcα-

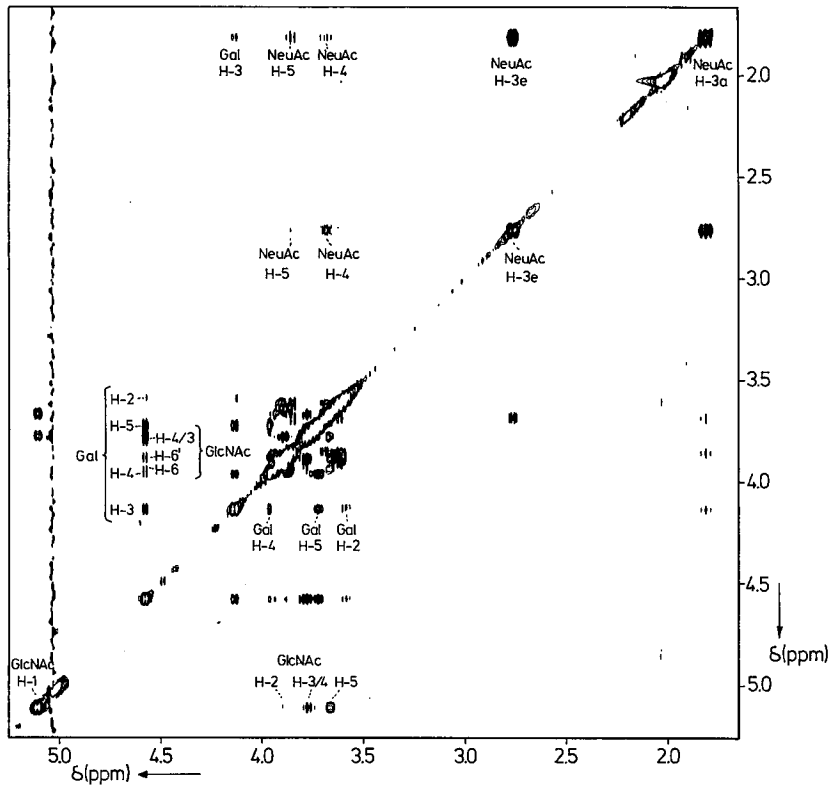

Fig. 8. *500-MHz NOESY spectrum at 4 °C of compound II with a mixing period of 0.45 s.* A number of NOEs that have been mentioned in the text are below the lowest level of the contour plot

(2 → 3)Gal linkage in II are in accordance with those calculated for the same linkage in G_{M1} [5]; the energy levels are however different, i.e. 0 and 18.4 kJ/mol for G_{M1} conformations B and A, respectively.

The NOESY spectrum of II, obtained at 4 °C with a mixing time of 0.45 s, points to many dipolar interactions within each residue (see Fig. 8). No inter-residue dipolar connectivities are observed from the GlcNAc anomeric proton to Asn protons. From Gal H-1 to GlcNAc across the glycosidic linkage NOE crosspeaks are observed with H-4 (coinciding with H-3), H-5, H-6′ and H-6 (coinciding with Gal H-4). Gal H-3 has inter-residue dipolar interactions with NeuAc H-3e, H-3a and H-8. Both NeuAc H-3e and H-3a display NOEs with Gal H-3 and H-4, while an additional effect is present between H-3a and Gal H-1. Gal H-4 overlaps with GlcNAc H-6 and the NOEs at $\delta = 3.863$ ppm and 3.661 ppm are ascribed to those from the latter proton to its H-6′ and H-5, respectively. The NOEs from Gal H-4 can be expressed as a percentage of the total Gal H-4 signal, by estimating the contribution of GlcNAc H-6 to the composite GlcNAc H-6/Gal H-4 diagonal peak from the intensity of the GlcNAc H-6′ crosspeak, compared to the mutual NOE crosspeak intensity between NeuAc H-3e and H-3a.

The influence of the overall conformation on the calculated intra-residue NOEs is within the error of the measurements. The ^{13}C relaxation data suggest τ_c to be 0.44 ns, but with this value the calculated intensities of NOEs between intra-residue ^1H-^1H pairs are only about one third of those observed. However, with $\tau_c = 1.1 \pm 0.3$ ns the crosspeak intensities are optimally reproduced at all three mixing times (Δ $rms_w \approx 0.9\%$). In these calculations no attempt has been made to differentiate between different parts of the molecule. The conformations of the two glycosidic linkages in II are then estimated from the interglycosidic NOEs using $\tau_c =$ 1.1 ns. The conformation of the Galβ(1 → 4)GlcNAc linkage can not be calculated directly from the NOE data, because GlcNAc H-3 and H-4 nearly coincide, precluding separate measurement of the NOEs between these protons and Gal H-1. Furthermore, due to strong coupling between GlcNAc H-3 and H-4, NOEs on either of these protons are partly relayed to the other [38]. The calculated crosspeak intensities for a Galβ(1 → 4)GlcNAc linkage with $\phi/\psi = 55°/5°$, as indicated by the HSEA calculations are however in good agreement with those observed for II (see Table 4).

For the NeuAcα(2 → 3)Gal linkage, with τ_c in the range 1.1 ± 0.3 ns, no minimum-energy conformation supported by either the HSEA or the MM2HB calculations fits the observed NOE crosspeak intensities (see Table 4). The differences between the NOEs calculated for the conformations A and A′, B and B′ and C and C′ are only minimal. Therefore, in the following only the conformations A, B and C are considered in the analysis. For conformations B and C some strong inter-residue NOEs are calculated involving NeuAc H-8 and H-5 (see Table 4). Crosspeaks between Gal H-3 and NeuAc H-5 and between Gal H-5 and NeuAc H-8 are in the bulk region of the spectrum, but not distinct crosspeaks are present above the detection level. The crosspeak at the Gal H-4/NeuAc H-8 position can be ascribed to the intense NOE between GlcNAc H-6 and H-6′. These NOE crosspeaks involving NeuAc H-8 and H-5 are therefore assumed to be 0, but the error in the observed intensity is taken much larger. The observed NOEs may be interpreted as the result of a single conformation or as the result of a distribution over more conformations. In a 5° grid search for a single conformation that fits the observed NOEs across the α(2 → 3)-linkage, an optimum is found at $\phi = 210 \pm 5°$ and $\psi = 10 \pm 5°$, with $\Delta rms_w = 0.5\%$ (see

Table 4. *Interglycosidic NOE crosspeak intensities for the NeuAcα(2→3)Galβ linkage in II at a mixing time of 0.45 s*
Compared are the observed and the calculated intensities at the various energy minima

Diagonal peak	Cross peak	Observed intensity	Calculated intensity for minimum energy conformation					
			A	A′	B	B′	C	C′
Gal H-3	NeuAc H-3e	1.6	0.3	0.3	4.5	4.0	0.4	0.5
Gal H-3	NeuAc H-3a	3.4	0.3	0.3	10.6	9.7	0.7	1.0
Gal H-3	NeuAc H-5	0[a]	0.2	0.1	2.7	2.7	0.5	0.5
Gal H-3	NeuAc H-8	2.0	5.4	3.1	0.9	0.9	4.0	4.0
Gal H-4	NeuAc H-6	0.0	0.1	0.1	0.4	0.4	0.9	1.1
Gal H-4	NeuAc H-8	0	0.5	0.3	7.8	10.2	9.0	8.7
Gal H-5	NeuAc H-8	0[b]	0.7	0.3	0.7	0.7	4.3	7.3
NeuAc H-3e	Gal H-3	1.3	0.3	0.3	5.2	4.8	0.5	0.6
NeuAc H-3e	Gal H-4	0.5	0.2	0.3	0.5	0.4	0.2	0.2
NeuAc H-3a	Gal H-1	0.6	0.1	0.0	1.1	0.8	0.1	0.1
NeuAc H-3a	Gal H-3	4.1	0.4	0.4	12.8	12.2	0.8	1.3
NeuAc H-3a	Gal H-4	0.5	0.2	0.2	1.3	1.0	0.2	0.3
NeuAc H-3a	Gal H-5	0[c]	0.1	0.1	1.0	0.7	0.1	0.1
Gal H-1	GlcNAc H-3		0.5	0.5	0.5	0.5	0.5	0.5
Gal H-1	GlcNAc H-4	13.7[d]	8.9	8.9	8.9	8.9	8.9	8.9
Gal H-1	GlcNAc H-5	1.3	0.9	0.9	0.9	0.9	0.9	0.9
Gal H-1	GlcNAc H-6′	3.8	3.8	3.8	3.8	3.8	3.8	3.8
Gal H-1	GlcNAc H-6		1.5	1.5	1.5	1.5	1.5	1.5
Δrms_w			0.8		1.9		1.1	

[a] No signal present at this cross-position.
[b] No signal present at this cross-position exceeding 0.3%.
[c] Not detected due to overlap.
[d] Composite signal of GlcNAc H-3 and H-4.

Table 5). At this single conformation however, both the HSEA and MM2HB approach indicate strong steric repulsion and energies higher than 42 kJ/mol, relative to the minima. Alternatively, the observed NOEs may be conceived as the result of a distribution over the energetically preferred orientations A, B and C. Indeed, a distribution amont the preferred conformations with 25% of B and 75% of A and/or C equally well reproduces the observed NOEs, with Δrms_w between 0.4–0.9% (see Table 5). Compared to the Δrms_w for the intraresidue NOEs, no further detailed analysis is justified, but the presence of a mixture of two or three preferred orientations is firmly established.

Conformation of III, with NeuAc in α(2→6)-linkage

The NOESY spectrum of III with a mixing time of 0.4 s (Fig. 9) displays a large number of intra-residue NOEs for Gal and GlcNAc, that are highly comparable to those observed for II. Unfortunately, the inter-residue NOE crosspeak intensities from Gal H-1 across the 1→4 linkage are difficult to quantify due to considerable overlap of Gal and GlcNAc signals, i.e. GlcNAc H-6 and H-6′ coincide with Gal H-4 and H-5, respectively, while GlcNAc H-4 and H-5 both almost coincide with Gal H-3. The intensities of the composite inter-/intra-residue crosspeaks are in close correspondence with those observed for II. The NOE experiment therefore points to a conformation for the Galβ(1→4)GlcNAc-linkage in III, that is not significantly different from that for II.

The overall conformation of III is to a great extent determined by the orientation around the Gal C-5–C-6 bond. The $J_{5,6}$ and $J_{5,6'}$ coupling constants are supportive of the *gt* orientation; a definitive proof for this orientation is obtained from Gal intra-residue NOEs. In the *gt* conformation Gal H-6 and H-6′ are at 0.252 nm and 0.321 nm, respectively, from Gal H-4, while for the *tg* orientation these values are 0.382 nm and 0.309 nm, respectively. The crosspeak between Gal H-6 and Gal H-4 is therefore decisive for the *gt* or *tg* orientation. Gal H-6 coincides with its H-2 and with NeuAc H-7, precluding measurement of the NOE crosspeak intensities as a percentage of the total signal. However, the Gal H-6/H-6′ and the Gal H-6/H-4 crosspeaks are unperturbed by other crosspeaks. In consequency, the intensity ratio of these two crosspeaks is straightforwardly determined from the spectrum as 3.4. The ratios that are calculated for the *gt* and the *tg* orientation are 5.3 and 23.3, respectively, confirming independently from earlier considerations the *gt* orientation.

For III no interglycosidic NOEs are detected between NeuAc and the rest of the molecule, precluding the deduction of a specific conformation for the 2→6 linkage. HSEA energy calculations for the completion of III by introducing NeuAc in α(2→6) linkage to Gal in I indicate that a small influence is possible for NeuAc on the position of the energy minimum for the (1→4) linkage. To comply with this interaction, ϕ/ψ for that linkage in III is taken as 60°/0. The ϕ/ψ energy profile for the α(2→6) linkage shows the presence of an extended low-energy surface with a number of local minimum-energy conformations, denoted A, B, C, D and E (see Fig. 10). The energy profile suggests that a distribution among many different conformations is allowed without severe steric repulsions. In conformation A the *N*-acetyl groups of NeuAc and GlcNAc are close to one another, with the distance between the carbonyl oxygen atoms being 0.265 nm. We consider this unrealistically short distance to be a result of the short oxygen van der Waal's radius used in the HSEA format which causes an overestimation of the stabilizing energy for this conformation.

Each of the conformations A–E support some NOEs. For conformations D and E strong inter-residue effects are

Table 5. *Interglycosidic NOE crosspeak intensities for the NeuAcα(2→3)Galβ linkage in II at a mixing time of 0.45 s* Observed and calculated NOE-intensities for optimized conformations

Diagonal peak	Cross peak	Observed intensity	Calculated intensity for conformations		
			$\phi/\psi = 210°/10°$	A:B = 0.75:0.25	B:C = 0.25:0.75
Gal H-3	NeuAc H-3e	1.6	1.2	1.4	1.5
Gal H-3	NeuAc H-3a	3.4	2.6	3.4	3.7
Gal H-3	NeuAc H-5	0[a]	1.6	0.9	1.1
Gal H-3	NeuAc H-8	2.0	1.4	4.2	3.2
Gal H-4	NeuAc H-6	0.0	0.2	0.2	0.8
Gal H-4	NeuAc H-8	0	1.8	2.4	8.7
Gal H-5	NeuAc H-8	0[b]	0.5	0.7	3.5
NeuAc H-3e	Gal H-3	1.3	1.5	1.8	1.9
NeuAc H-3e	Gal H-4	0.5	0.2	0.3	0.3
NeuAc H-3a	Gal H-1	0.6	0.5	0.3	0.4
NeuAc H-3a	Gal H-3	4.1	3.3	4.2	4.5
NeuAc H-3a	Gal H-4	0.5	0.4	0.5	0.5
NeuAc H-3a	Gal H-5	0[c]	0.3	0.3	0.4
Δrms_w			0.5	0.4	0.9

[a] No signal present at this cross-position.
[b] No signal present at this cross-position exceeding 0.3%.
[c] Not detected due to overlap.

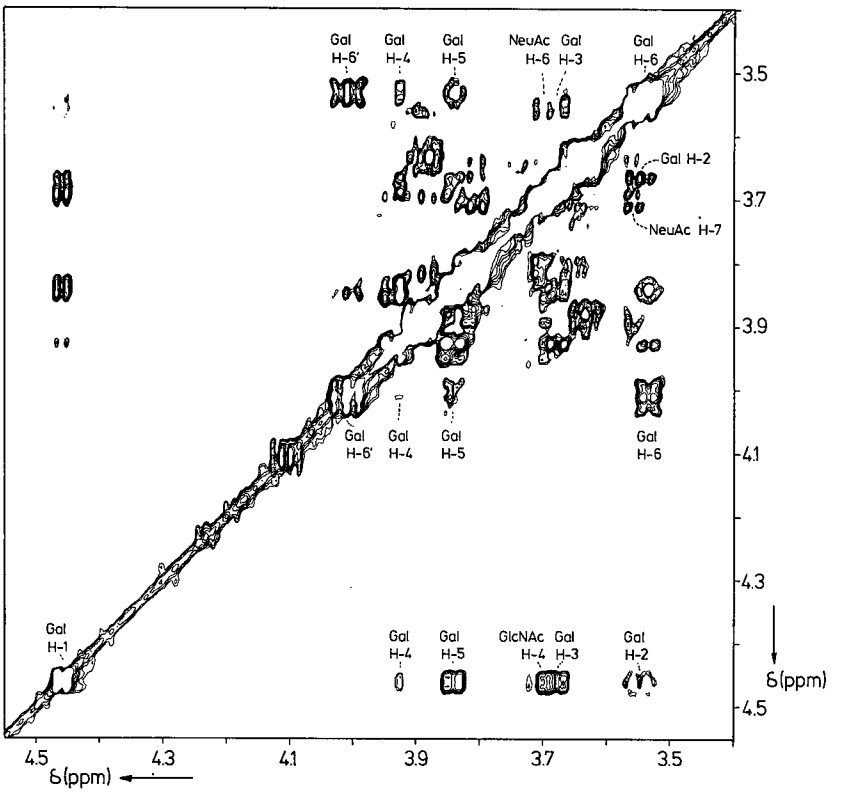

Fig. 9. *500-MHz NOESY spectrum of III obtained at 5°C and with a mixing time of 0.4 s.* Only a limited number of NOE crosspeaks are assigned in the figure

calculated between Gal H-6 and H-6′ and NeuAc H-3a and H-3e, with intensities varying between 5−10%. For conformation C intense crosspeaks are expected between NeuAc H-8 and nearly all protons of Gal (intensities up to 10%), while for conformations A and B only inter-residue NOEs are expected between Gal H-6 and H-6′ and NeuAc H-8 (up to 5%). A mixture of conformations with equal contributions of A, B, C, D and E generates NOE intensities between the Gal H-6 and NeuAc H-3 protons with intensities varying between 1−4%, together with NOEs between NeuAc H-8 on the one side and Gal H-3, H-4 and H-5 on the other of 1−4%. The ^{13}C T_1 relaxation data do not indicate an increased motion of the C-6 hydroxymethyl group of Gal with respect to the remaining Gal skeleton, but a jump motion between the different energy minima will still be present. This may reduce the NOEs across the glycosidic linkage. For protons that are close

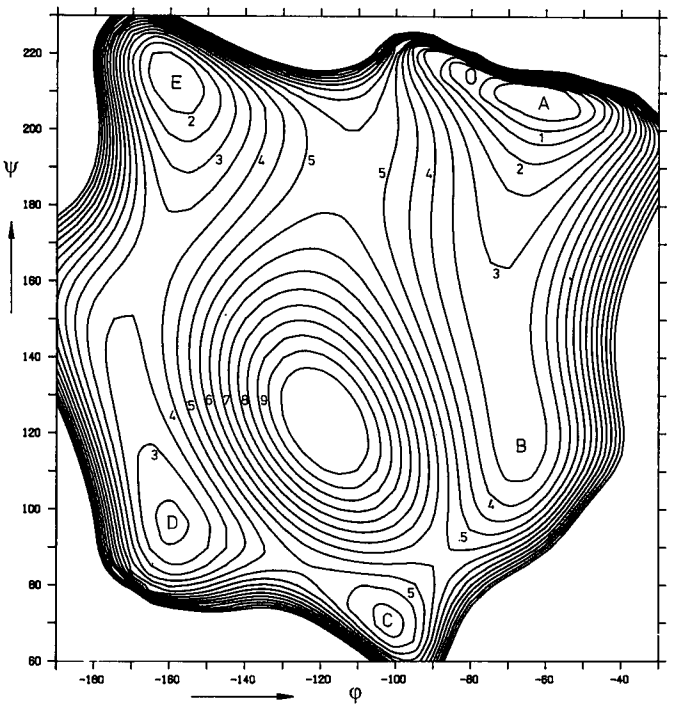

Fig. 10. *Energy profile calculated according to the HSEA format for part of the* ϕ/ψ *space connected with the NeuAcα(2→6)Gal linkage for III.* The indicated levels are 0.5 kcal/mol (2.1 kJ/mol) apart and energies more than 10 kcal/mol (42 kJ/mol) above the minimum have been omitted

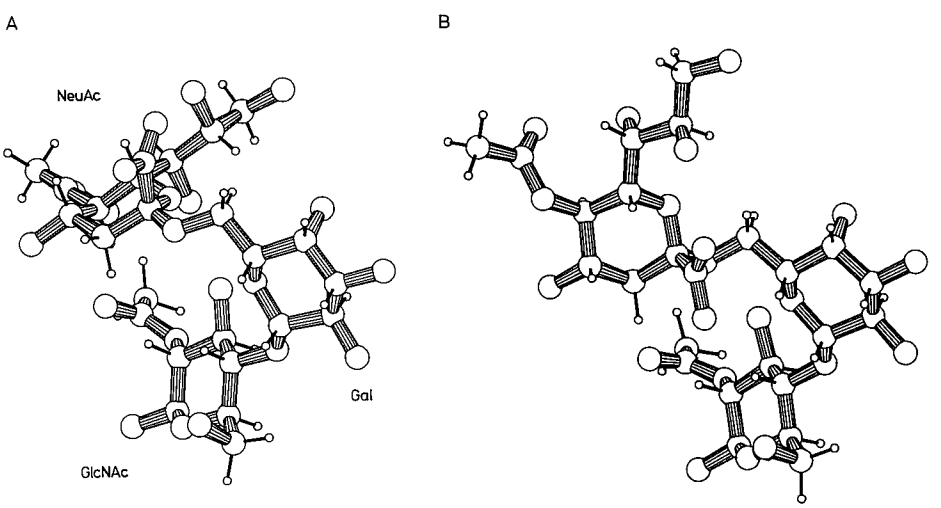

Fig. 11. *Conformations of compound III calculated using the HSEA energy format and supported by the NOE data.* For the $\beta(1\rightarrow4)$ linkage, $\phi/\psi = 60°/0$ and for the $\alpha(2\rightarrow6)$-linkage, $\phi/\psi = -60°/210°$ (A) or $-70°/120°$ (B). Asn has been omitted from the figure

to the glycosidic linkage, such motion would be the smallest. Consequently, significant contributions of conformations D and E are excluded. The remaining conformations, especially A and B, are consistent with a more-or-less folded overall conformation (see Fig. 11). A less pronounced energy minimum for conformation A would provide an extended shallow low-energy region combining A and B. A further increased motion within the NMR time scale for this conformation region, with an increase of the effective τ_c for the interglycosidic NOEs involving NeuAc H-8, would reduce the intensity of the interglycosidic NOEs associated with conformations A and B. An overall folded conformation of III (see Fig. 11), would provide a mechanism for the previously mentioned NeuAc-induced long-range chemical-shift effects on GlcNAc, i.e. shift effects induced by steric interactions and/or deshielding by oxygen atoms. In the folded conformation of III, NeuAc O-6 is close to Gal H-6′ and not to Gal H-6; the concomitant deshielding coincides with the opposite shift effects for these protons upon attachment of NeuAc. A steric interaction between NeuAc and GlcNAc of III would possibly result in a change of the orientation of the Gal$\beta(1\rightarrow4)$GlcNAc linkage, but whether this actually is the case can not be determined from the NOE data.

Conclusions

For low amounts of material a prolonged mixing time is needed in a NOESY experiment to obtain sufficient NOE-crosspeak intensity. This makes the use of the full relaxation matrix obligatory. For molecules for which the product of

spectrometer angular frequency (ω_0) and τ_c is near unity, the NOEs are equally small, providing even more reason to use a prolonged mixing time. In the latter case the crosspeak intensities are however greatly influenced by τ_c. The value of τ_c determined from ^{13}C-NMR relaxation data does not suffice in the present analysis. This may be the result of an actual anisotropic overall motion of II (and III), not accounted for in the analysis, combined with slightly differing τ_c values for different parts of the molecule. It is therefore more appropriate to calibrate τ_c using intra-residue NOE crosspeaks. A prolonged mixing time counteracts the precision of the latter, due to relayed NOEs from conformation-dependent interglycosidic NOE crosspeak intensities. This might account for the large residual standard deviation between observed and calculated crosspeaks for II. Despite these limitations, the present analysis firmly establishes the presence of multiple conformations for the 2→3 linkage in the NeuAcα(2→3)Galβ(1→4)GlcNAcβ structural element. An averaging of NOEs due to a distribution among two different states has been described before for the Galα(1→4)Gal linkage in a glycolipid head group [18]. A further refinement of the calculated NOE crosspeak intensities might be obtained by an ensemble-averaged relaxation matrix [39], although such might reach beyond the quality of the NOE data and the limitations of the energy functions. For the structural element NeuAcα(2→6)Galβ(1→4)GlcNAcβ a folded overall conformation is suggested, based on the unequivocal *gt* orientation of the Gal C-5–C-6 bond. The latter conformation provides an explanation for the shift effects observed for this structural element.

The analysis was hampered by the frequent occurrence of spectral overlap, sometimes resulting in strong coupling. These are common features for oligosaccharides and no straightforward solution is available. The presently used model for calculating the NOEs does not include these strong coupling effects; neither does it account for possible anisotropic rotation and different τ_c values for different parts of the molecules. A further refinement of the model, including these features, may be necessary to analyse NOESY spectra more accurately. For the compounds that were used in the present study, the quantitative analysis of the NOESY spectra was hampered by an unfavourable value of $\omega_0\tau_c$. It may prove better for these small oligosaccharides to measure the NOEs in the rotating frame (ROESY), for which the effects are much less dependent on τ_c [40]. The quantitative interpretation of ROESY data is, however, still hampered by the occurrence of coherent and non-coherent magnetization transfer in the same type of experiment [41]. In favourable cases, for larger oligosaccharides and glycopeptides a quantitative analysis using NOESY spectroscopy is still feasible.

Thanks are due to Dr H. van Halbeek for stimulating discussions in the initial phase of this work and to Dr K. Bock for recording the ^{13}C-NMR spectrum of compound III.

REFERENCES

1. Reutter, W., Köttgen, E., Bauer, C. & Gerok, W. (1982) in *Sialic acids – chemistry, metabolism and functions* (Schauer, R., ed.) pp. 263–305, Springer-Verlag, Wien.
2. Schauer, R. (1982) *Adv. Carbohydr. Chem. Biochem. 40*, 132–234.
3. Vliegenthart, J. F. G., Dorland, L. & Van Halbeek, H. (1983) *Adv. Carbohydr. Chem. Biochem. 41*, 209–374.
4. Vliegenthart, J. F. G., Van Halbeek, H. & Dorland, L. (1981) *Pure Appl. Chem. 53*, 45–77.
5. Sabesan, S., Bock, K. & Lemieux, R. U. (1984) *Can. J. Chem. 62*, 1034–1045.
6. Richarz, R. & Wüthrich, K. (1978) *J. Magn. Reson. 30*, 147–150.
7. Michalski, J.-C. (1984) Thesis, Université de Sciences et Techniques de Lille I.
8. Bodenhausen, G., Freeman, R., Morris, G. A. & Turner, D. L. (1978) *J. Magn. Reson. 31*, 75–95.
9. Nagayama, K., Bachmann, P., Wüthrich, K. & Ernst, R. R. (1978) *J. Magn. Reson. 31*, 133–148.
10. Haasnoot, C. A. G. (1983) *J. Magn. Reson. 52*, 153–158.
11. Rance, M., Sørensen, O. W., Bodenhausen, G., Wagner, G., Ernst, R. R. & Wüthrich, K. (1983) *Biochem. Biophys. Res. Commun. 117*, 479–489.
12. Marion, D. & Wüthrich, K. (1983) *Biochem. Biophys. Res. Commun. 113*, 967–974.
13. Macura, S. & Ernst, R. R. (1980) Mol. Phys *41*, 95–117.
14. Kumar, A., Ernst, R. R. & Wüthrich, K. (1980) *Biochem. Biophys. Res. Commun. 95*, 1–6.
15. Macura, S. Huang, Y., Suter, D. & Ernst, R. R. (1981) *J. Magn. Reson. 43*, 259–281.
16. Vold, R. L., Waugh, L. S., Klein, M. P. & Phelps, D. E. (1968) *J. Chem. Phys. 48*, 3831–3832.
17. Kuhlmann, K. F., Grant, D. M. & Harris, R. K. (1970) *J. Chem. Phys. 52*, 3439–3448.
18. Scarsdale, J. N., Yu, R. K. & Prestegard, J. H. (1986) *J. Am. Chem. Soc. 108*, 6778–6784.
19. Keepers, J. W. & James, T. L. (1984) *J. Magn. Reson. 57*, 404–426.
20. Lemieux, R. U., Bock, K., Delbaere, L. T. J., Koto, S. & Rao, V. S. (1980) *Can. J. Chem. 58*, 631–653.
21. Kitaygorodsky, A. I. (1978) *Chem. Soc. Rev. 7*, 133–162.
22. Thögersen, H., Lemieux, R. U., Bock, K. & Meyer, B. (1982) *Can. J. Chem. 60*, 44–57.
23. Takagi, S. & Jeffrey, G. A. (1979) *Acta Crystallogr. B35*, 902–906.
24. Mo, F. (1979) *Acta Chem. Scand. A33*, 207–218.
25. Reference deleted.
26. Brown, E. B., Brey, W. S. Jr & Weltner, W. Jr (1975) *Biochem. Biophys. Acta 399*, 124–130.
27. Allinger, N. L. & Yuh. Y. H. (1980) *Quantum chemistry program exchange*, no. 423, Chemistry Department, Indiana University, Bloomington, IN.
28. Kroon-Batenburg, J. M. L. & Kanters, J. A. (1983) *J. Mol. Struct. (Theochem) 105*, 417–425.
29. Brisson, J.-R. & Carver, J. (1982) *J. Biol. Chem. 257*, 11207–11209.
30. Haasnoot, C. A. G., Leeuw, F. A. A. M. de, & Altona, C. (1980) *Tetrahedron 36*, 2783–2792.
31. Ohrui, H., Nishida, Y., Higuchi, H., Hori, H. & Meguro, H. (1987) *Can. J. Chem. 65*, 1145–1153.
32. Nishida, Y., Hori, H., Ohrui, H. & Meguro, H. (1987) *Carbohydr. Res. 170*, 106–111.
33. Berman, E. (1984) *Biochemistry 23*, 3754–3759.
34. Dijkstra, B. W., Vliegenthart, J. F. G., Strecker, G. & Montreuil, J. (1983) *Eur. J. Biochem. 130*, 111–115.
35. Wüthrich, K. (1976) *NMR in biological research*, North-Holland Publishing Company, Amsterdam.
36. Jaques, L. W., Glant, S. & Weltner, W. Jr (1980) *Carbohydr. Res. 80*, 207–211.
37. Czarniecki, M. F. & Thornton, E. R. (1977) *J. Am. Chem. Soc.* 99, 8273–8279.
38. Kay, L. E., Scarsdale, J. N., Hare, D. R. & Prestegard, J. H. (1986) *J. Magn. Reson. 68*, 515–525.
39. Cumming, D. A. & Carver, J. P. (1987) *Biochemistry 26*, 6664–6676.
40. Bothner-By, A. A., Stephens, R. L. & Lee, J.-M. (1984) *J. Am. Chem. Soc. 106*, 811–813.
41. Bax, A. & Davis, D. G. (1985) *J. Magn. Reson. 63*, 207–213.